Journal of Physics: Conference Series **485** (2014) 012034 doi:10.1088/1742-6596/485/1/012034

Cosmic-ray and gamma-ray constraints on dark matter stability

David Tran

School of Physics and Astronomy, University of Minnesota
116 Church Street SE, Minneapolis, MN 55455, USA

E-mail: tran@physics.umn.edu

Abstract. We examine different constraints on dark matter stability from cosmic-ray and gamma-ray observations and their complementarity through higher-order effects. Two-body and three-body decays of dark matter particles into charged leptons and quarks generically induce decays into monochromatic photons at the quantum level, giving rise to distinct signatures. We also present a general model-independent analysis of hadronic constraints in the mass-lifetime parameter space and compare those constraints to current and projected limits on gamma-ray lines. Furthermore, we discuss how the production of monochromatic photons can be enhanced by kinematic effects, potentially giving rise to observable lines in the gamma-ray sky.

1. Introduction

The existence of a substantial quantity of dark matter in the Universe is now established beyond reasonable doubt. Nevertheless, the physical identity of the dark matter remains mysterious. While we do know that the dark matter cannot be composed of Standard Model particles, little is known about the microscopic properties of the particles that the dark matter is made of. Among the unknown properties of the dark matter particles is their lifetime. From the observation of a population of primordial relic dark matter particles we can assume that the dark matter lifetime at the very least exceeds the age of the Universe. It is commonly assumed that the dark matter particles have infinite lifetime owing to to the effects of some stabilizing symmetry that prohibits the decay of dark matter into Standard Model or hidden-sector particles. Nevertheless, one should keep in mind that perfect dark matter stability is an unproved assumption. If the dark matter decays into Standard Model particles, one can derive from observations of cosmic-rays, photons and neutrinos much more stringent constraints on the partial decay widths, which typically exceed the age of the Universe by a factor of about 10^9. We examine two different types of constraints on unstable dark matter here, namely the hadronic constraints from measurements of the cosmic-ray antiproton spectrum as well as constraints from searches for gamma-ray lines, which may be generated at the loop-level by dark matter decay processes involving charged particles.

2. Gamma-Ray Lines from Radiative Dark Matter Decay

The observation of anomalous abundances of cosmic-ray positrons and electrons at high energies by the PAMELA [1] and Fermi LAT [2] cosmic-ray observatories has motivated many authors to study models of dark matter which self-annihilates or decays primarily or exclusively into leptons,

thus accounting for the excess high-energy electrons without simultaneously overproducing antiprotons. We investigate here a way to test such "leptophilic" models by examining some next-to-leading order effects induced by loop diagrams. To this end, we study a toy model of unstable dark matter which at leading order decays only into charged lepton–antilepton pairs (for scalar dark matter $\phi_{\rm DM}$) or into three-body final states including lepton–antilepton pairs plus neutral fermions N (due to angular momentum conservation in the case of fermionic dark matter $\psi_{\rm DM}$). One such diagram contributing to the leptonic decay of a dark matter fermion is shown in Fig. 1.

The external charged lepton lines can be closed into a loop from which a photon is radiated. In this way, a three-body decay can induce a radiative two-body decay at the quantum level. One diagram contributing to the one-loop decay process is shown in Fig. 2. We assume here that the decay is mediated either by a charged scalar Σ or a charged vector particle V, both of which are assumed to be much heavier than the dark matter particle so that these particles cannot be produced on-shell.

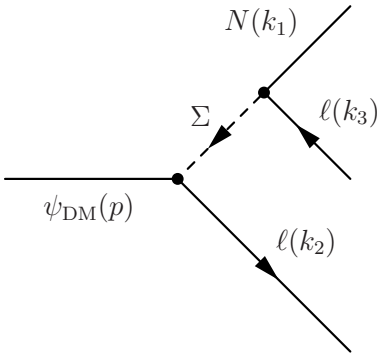

Figure 1. Tree-level diagram contributing to the three-body decay $\psi_{\rm DM} \to \ell^+\ell^-\nu$ of fermionic dark matter via a virtual scalar Σ.

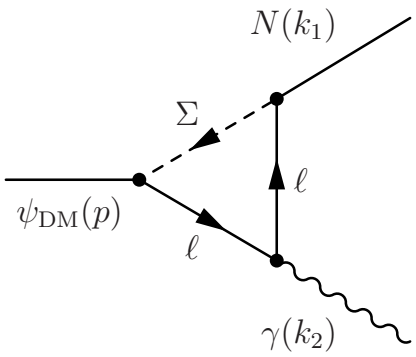

Figure 2. One-loop diagram contributing to the radiative two-body decay $\psi_{\rm DM} \to \gamma\nu$.

This subdominant two-body decay process then generates photons at a fixed energy

$$E_\gamma = \frac{m_{\psi_{\rm DM}}}{2}\left(1 - \frac{m_N^2}{m_{\psi_{\rm DM}}^2}\right), \tag{1}$$

or simply half the dark matter mass if the neutral particle N is massless.[1] For dark matter particles of roughly electroweak-scale mass these photons could conceivably show up as narrow lines in the diffuse Galactic gamma-ray emission or in the gamma-ray flux from certain astrophysical objects. Such gamma-ray lines are of great interest due to the fact that they cannot be produced by ordinary astrophysical processes. Therefore, the identification of a line in the gamma-ray spectrum would constitute a compelling signature of an underlying particle physics process.

General expressions for the tree-level and radiative decay modes of scalar and fermionic dark matter decaying leptonically via virtual scalar or vector particles can be found in [3]. For scalar dark matter we generally find that the decays into two photons are strongly chirality-suppressed by the hierarchy between lepton and dark matter masses, making the resulting lines

[1] We use the letter ν to denote a general massless neutral fermion.

unobservable in practice. For fermionic dark matter $\psi_{\rm DM}$, the prospects of detection are more promising. It is interesting to study special cases in which the expressions for the branching ratios assume relatively simple forms. For instance, if the decay is mediated by a virtual scalar and the couplings of the dark matter are chiral, the ratio between the radiative decay $\psi_{\rm DM} \to \gamma\nu$ and the tree-level three-body decay $\psi_{\rm DM} \to \ell^+\ell^-\nu$ can be expressed in a very simple manner,

$$\frac{\Gamma(\psi_{\rm DM} \to \gamma\nu)}{\Gamma(\psi_{\rm DM} \to \ell^+\ell^-\nu)} = \frac{3\alpha_{\rm em}}{8\pi} \times R \times S, \tag{2}$$

where R and S encode the details of the various coupling constants and the ratio between the two-body and three-body kinematic factors, respectively. For generic couplings, the corresponding factor R as well as the kinematic factor S are of order one. Therefore, the relative intensity of the radiative decay mode compared to the dominant tree-level decay is determined by the numerical prefactor $3\alpha_{\rm em}/8\pi \approx 10^{-3}$. We show our results for the gamma-ray line bounds induced by the leading-order flavor-democratic leptonic decay $\psi_{\rm DM} \to \ell^+\ell^-\nu$ in the case of chiral couplings in Figs. 3 and 4 for the decay mediated by a scalar and a vector. The relative intensity of the gamma-ray line is stronger by about an order of magnitude in the case of a vector-mediated decay. We show these bounds together with the region of the parameter space that yields an explanation of the cosmic-ray anomalies observed by PAMELA and Fermi LAT, shown here in yellow and gray, respectively, indicating the 3σ and 5σ regions around the best-fit points [4]. The observational constraints shown in the plot are from Fermi LAT line searches in the Galactic halo at lower energies [5], as well as from MAGIC observations of the Perseus galaxy cluster [6], HEGRA observations of M31 [7], as well as H.E.S.S. measurements of the diffuse electron flux [8], which provides an upper limit on the gamma-ray flux. We also show our projected limits for the future Cherenkov Telescope Array (CTA). Interestingly enough, the existing Fermi LAT bounds at lower energies and the projected CTA limits at higher energies can constrain a significant portion of the parameter space relevant to dark matter interpretations of the anomalous cosmic-ray lepton abundances.

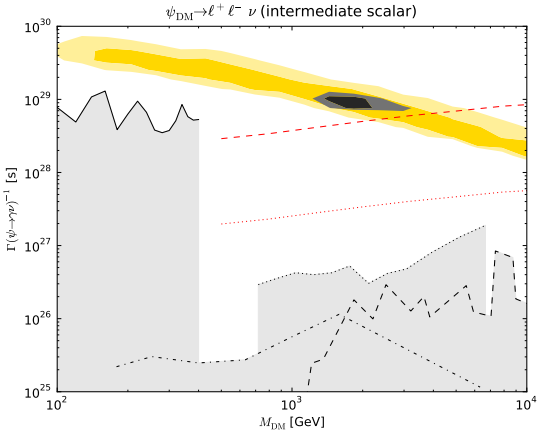

Figure 3. Gamma-ray line bounds on the radiative decay $\psi_{\rm DM} \to \gamma\nu$ induced by the tree-level decay $\psi_{\rm DM} \to \ell^+\ell^-\nu$, mediated by a virtual scalar particle.

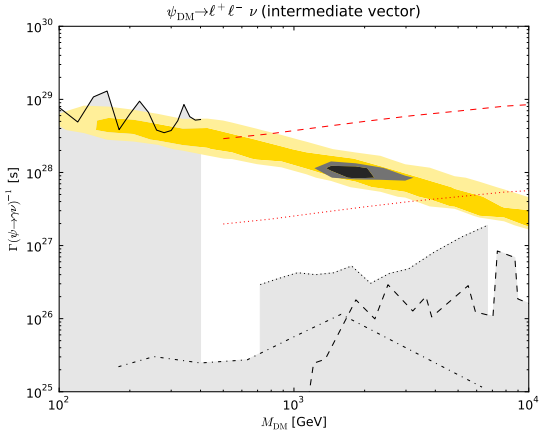

Figure 4. Gamma-ray line bounds on the radiative decay $\psi_{\rm DM} \to \gamma\nu$ induced by the tree-level decay $\psi_{\rm DM} \to \ell^+\ell^-\nu$, mediated by a virtual vector particle.

It is worth noting that if the neutral fermion N and the dark matter particle $\psi_{\rm DM}$ have

opposite CP parities the radiative decay mode can be enhanced due to a kinematic factor

$$\mathrm{BR}(\psi_{\mathrm{DM}} \to \gamma\nu) \propto \left(1 - \frac{m_N}{m_{\mathrm{DM}}}\right)^{-2} \tag{3}$$

in the branching ratio into monochromatic photons. Therefore, as $m_N \to m_{\psi_{\mathrm{DM}}}$ the radiative branching ratio can grow dramatically. Using this kinematic enhancement factor, one can construct scenarios where the constraints from the non-observation of gamma-ray lines are stronger than the ones from leptonic cosmic rays. We show a number of benchmark points representating different scenarios in Fig. 5. Depending on the relative masses of ψ_{DM} and N the benchmark points shown in the plot can lie within the allowed or excluded regions of the parameter space.

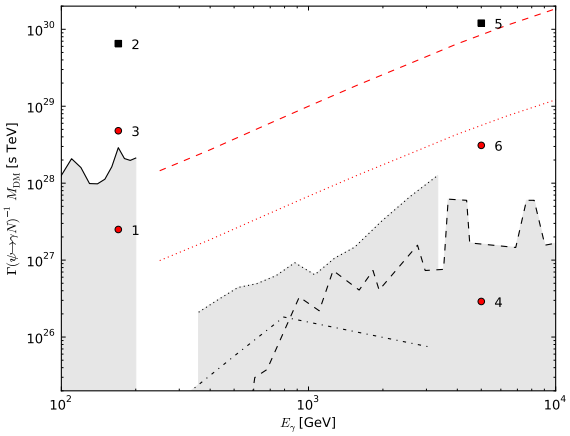

Figure 5. Benchmark points for the decay into $\psi_{\mathrm{DM}} \to \gamma N$ with a massive neutral fermion N and opposite CP parities of ψ_{DM} and N. Some benchmark points are excluded, allowed or borderline excluded. The constraints are rescaled compared to Figs. 3 and 4 due to the reduced gamma-ray energy available due to the non-zero mass of N.

3. Hadronic Constraints

If the dark matter decays into states involving weak gauge bosons, Higgs bosons or quarks, these particles will hadronize and generate antiprotons, which constitute a sensitive probe for the presence of primaries due to their scarcity in the cosmic radiation. The PAMELA cosmic-ray telescope has observed no deviations from the theoretically expected abundance of cosmic antiprotons if these particles are produced as secondary cosmic rays by spallation on interstellar gas. The absence of excess cosmic antiprotons over the predicted astrophysical flux from cosmic-ray spallation on interstellar gas can therefore be used to impose stringent constraints on hadronic dark matter decay modes. We utilize the recent PAMELA measurements of the antiproton-to-proton flux ratio [9] to derive limits on dark matter stability in various hadronic decay modes in a model-independent manner.

We model the propagation of charged cosmic rays in the Milky Way's magnetic halo using a stationary two-zone diffusion model with cylindrical boundary conditions [10]. This model takes into account the effects of diffusion, energy loss, convection and annihilation on interstellar gas.

Under certain assumptions, the resulting differential equation can be solved semi-analytically, with the solution depending on only a small number of parameters to be determined from cosmic-ray measurements. Using these solutions we can inject a source spectrum of antiprotons at a given rate and a spatial distribution as determined by N-body simulations. The determination of the free parameters of the transport model from cosmic-ray measurements suffers from a degeneracy between the size of the diffusion coefficient and the height of the diffusive halo. This degeneracy cannot be broken by measurements of stable secondary-to-primary cosmic-ray species which are only produced in the Galactic disk. However, since antiprotons from dark matter decay/annihilation are produced everywhere in the dark matter halo and not just in the disk, the flux of these primary antiprotons is highly sensitive to different configurations of the propagation parameters. The resulting primary antiproton fluxes can vary by as much as two orders of magnitude. Therefore, we show our constraints for the three different sets of transport parameters which correspond to minimum, medium and maximum antiproton flux.

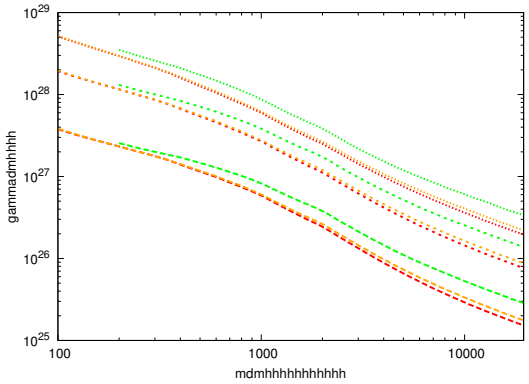

Figure 6. Lower bounds on the partial dark matter lifetime for fermionic dark matter decaying into weak gauge bosons or Higgs bosons. Red: $\psi_{\rm DM} \to W^{\pm}\ell^{\mp}$, orange: $\psi_{\rm DM} \to Z^0\nu$, green: $\psi_{\rm DM} \to h^0\nu$.

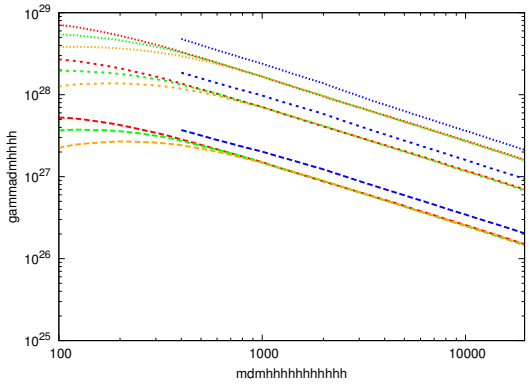

Figure 7. Lower bounds on the partial dark matter lifetime for fermionic dark matter decaying into quark–antiquark pairs and a neutral fermion. Red: $\psi_{\rm DM} \to d\bar{d}\nu$, green: $\psi_{\rm DM} \to c\bar{c}\nu$, orange: $\psi_{\rm DM} \to s\bar{s}\nu$, blue: $\psi_{\rm DM} \to t\bar{t}\nu$.

We have computed exclusion limits on various hadronic decay modes of dark matter from the requirement of not exceeding the antiproton-to-proton ratio observed by PAMELA at 95% C.L. To this end, we scanned over several orders of magnitude in the dark matter mass and lifetime. The resulting constraints on a wide range of general hadronic dark matter decay modes allowed by charge and angular momentum conservation are shown in [11]. As an example, we show in Figs. 6 and 7 the constraints on the mass–lifetime parameter space we find for the decay of a spin-1/2 dark matter particle into weak gauge bosons/Higgs bosons and into quark–antiquark pairs plus neutral fermions, respectively. Different line styles correspond to different sets of transport parameters as explained above.

Going beyond the cosmic-ray constraints, we can examine the radiative decays into monoenergetic photons in analogy to the previous section, where the photons are radiated from quark loops instead of lepton loops here. It is interesting to see how the constraints from gamma-ray line searches compare to the constraints on hadronic cosmic rays. We show our results for the cosmic-ray limits on the decay of fermionic dark matter via $\psi_{\rm DM} \to d\bar{d}\nu$ in Figs. 8 and 9 together with the gamma-ray line constraints from Fermi LAT and the projected limits for the CTA mentioned in the previous section (limits on the signal + astrophysical background flux

are shown in thick lines, whereas limits on the dark matter signal alone are shown in thin lines). While the antiproton constraints are stronger as expected, the complementary constraints from the radiative next-to-leading order decays provide a model-independent alternative view of the highly model-dependent hadronic constraints. The same kinematic enhancement effect that we mentioned in the previous section can also lead to a significant relative enhancement of the strength of the radiative constraints.

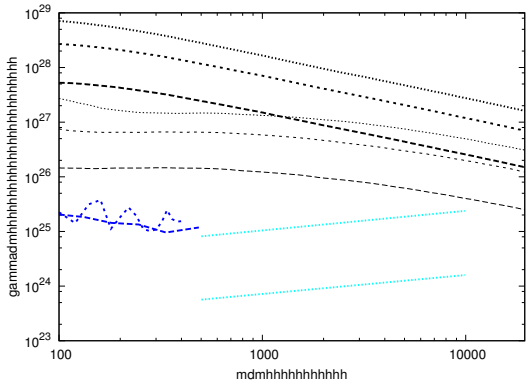

Figure 8. Comparison between hadronic constraints for the decay $\psi_{\rm DM} \to d\bar{d}\nu$ and gamma-ray line constraints from monochromatic photons radiated off of down-quark loops. Constraints shown for a decay mediated by an intermediate scalar.

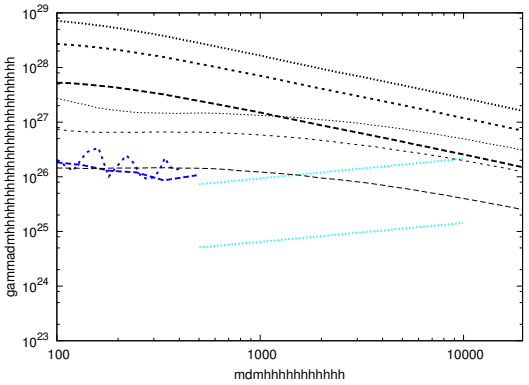

Figure 9. Comparison between hadronic constraints for the decay $\psi_{\rm DM} \to d\bar{d}\nu$ and gamma-ray line constraints from monochromatic photons radiated off of down-quark loops. Constraints shown for a decay mediated by an intermediate vector.

4. Conclusions

We have presented general constraints on dark matter stability from observations of gamma rays and cosmic-ray antiprotons. Using cosmic-ray antiproton measurements we have derived general constraints on hadronic dark matter decay modes and explored the complementarity with gamma-ray line constraints from subdominant quantum-level processes which can arise in any scenario where the dark matter decays into charged particles. We have explained that such processes can be relevant despite a general suppression by small couplings and loop factors compared to the leading-order decays.

References

[1] Adriani O *et al.* (PAMELA Collaboration) 2009 *Nature* **458** 607 (*Preprint* 0810.4995 [astro-ph])
[2] Ackermann M *et al.* (Fermi LAT Collaboration] 2010 *Phys. Rev.* **D82** 092004 (*Preprint* 1008.3999 [astro-ph.HE]).
[3] Garny M, Ibarra A, Tran D and Weniger C 2011 *JCAP* **1101** 032 (*Preprint* 1011.3786 [hep-ph])
[4] Ibarra A, Tran D and Weniger C 2010 *JCAP* **1001** 009 (*Preprint* 0906.1571 [hep-ph])
[5] Abdo A A, Ackermann M, Ajello M, Atwood W B, Baldini L, Ballet J, Barbiellini G and Bastieri D *et al.* 2010 *Phys. Rev. Lett.* **104** 091302 (*Preprint* 1001.4836 [astro-ph.HE])
[6] Aleksic J *et al.* (MAGIC Collaboration) 2010 *Astrophys. J.* **710** 634 (*Preprint* 0909.3267 [astro-ph.HE])
[7] Aharonian F A *et al.* (HEGRA Collaboration) 2003 *Astron. Astrophys.* **400** 153 (*Preprint* astro-ph/0302347).
[8] Aharonian F A *et al.* (H.E.S.S. Collaboration) 2008 *Phys. Rev. Lett.* **101** 261104 (*Preprint* 0811.3894 [astro-ph])
[9] Adriani O *et al.* (PAMELA Collaboration) 2010 *Phys. Rev. Lett.* **105** 121101 (*Preprint* 1007.0821 [astro-ph.HE])
[10] *See, for example,* Berezinskii V S, Buolanov S V, Dogiel V A, Ginzburg V L and Ptuskin V S 1990 "Astrophysics of Cosmic Rays" (Amsterdam: North–Holland)
[11] Garny M , Ibarra A and Tran D 2012 *JCAP* **1208** 025 (*Preprint* 1205.6783 [hep-ph])